HOKKAIDO UNIVERSITY

Title	Ozone variations over the northern subtropical region revealed by ozonesonde observations in Hanoi
Author(s)	Ogino, S.-Y.; Fujiwara, M.; Shiotani, M. et al.
Citation	Journal of Geophysical Research: Atmospheres, 118(8), 3245-3257 https://doi.org/10.1002/jgrd.50348
Issue Date	2013-04-27
Doc URL	https://hdl.handle.net/2115/64747
Rights	Copyright 2013 American Geophysical Union.
Type	journal article
File Information	Ogino_et_al-2013-Journal_of_Geophysical_Research__Atmospheres.pdf



Hokkaido University Collection of Scholarly and Academic Papers : HUSCAP

JOURNAL OF GEOPHYSICAL RESEARCH: ATMOSPHERES, VOL. 118, 3245–3257, doi:10.1002/jgrd.50348, 2013

Ozone variations over the northern subtropical region revealed by ozonesonde observations in Hanoi

S.-Y. Ogino,[1,2] M. Fujiwara,[3] M. Shiotani,[4] F. Hasebe,[3] J. Matsumoto,[1,5]
Thuy Ha T. Hoang,[6] and Tan Thanh T. Nguyen[6]

Received 4 December 2012; revised 15 March 2013; accepted 19 March 2013; published 30 April 2013.

[1] Seasonal and subseasonal variations in the ozone mixing ratio (OMR) are investigated by using continuous 7 year ozonesonde data from Hanoi (21°N, 106°E), Vietnam. The mean seasonal variations for the 7 years show large amplitude at the upper troposphere and lower stratosphere (UTLS) region (10–18 km) and at the lower troposphere (around 3 km) with standard deviations normalized by the annual mean value of about 30% for both regions. In the UTLS region, the seasonal variation in the OMR shows a minimum in winter and a maximum in spring to summer. The variation seems to be caused by the seasonal change in horizontal transport. Low OMR air masses are transported from the equatorial troposphere in winter by the anticyclonic flow associated with the equatorial convections, and high OMR air masses are transported from the midlatitude stratosphere in summer possibly due to Rossby wave breakings in the UT region and anticyclonic circulation associated with the Tibetan High in the LS region. In the lower troposphere, a spring maximum is found at 3 km height. Biomass burning and tropopause foldings are suggested as possible causes of this maximum. Subseasonal variations in the OMR show large amplitude in the UTLS region (at around 15 km) and in the boundary layer (below 1 km) with the standard deviations normalized by the annual mean larger than 40%. The OMR variations in the winter UTLS region have a negative correlation with the meridional wind. This relation indicates that the low OMRs observed at Hanoi has been transported from the equatorial region.

Citation: Ogino, S.-Y., M. Fujiwara, M. Shiotani, F. Hasebe, J. Matsumoto, T. H. T. Hoang, and T. T. T. Nguyen (2013), Ozone variations over the northern subtropical region revealed by ozonesonde observations in Hanoi, *J. Geophys. Res. Atmos.*, *118*, 3245–3257, doi:10.1002/jgrd.50348.

1. Introduction

[2] Atmospheric ozone is a gas that has activity in both infrared and ultraviolet-visible regions. In the stratosphere, heating due to ultraviolet absorption by the ozone has an essential role in determining the basic atmospheric structure. In the troposphere, ozone controls the air quality by producing OH radical and works as a greenhouse gas [e.g., *Brasseur et al*., 2003]. Recently, it was shown that the tropospheric ozone is increasing (positive radiative forcing) and contributes to the global warming [*Solomon et al.*, 2007]. However, the observations show that the ozone variation has strong dependence on location. In recent decades, increasing ozone mixing ratios were observed in high latitudes [e.g., *Tarasick et al*., 2005], whereas a decrease was observed over Europe and North America [*Logan et al*., 2012]. In the stratosphere, it is reported that the ozone amount had a negative trend until the 1990s and is slightly increasing in recent years [*WMO*, 2011]. The stratospheric ozone decrease gives both positive radiative effect due to an increase in solar radiation reaching the troposphere and negative one due to a decrease in thermal infrared emission, and the consequent radiative balance is sensitive to the vertical distribution of ozone depletion [*Shine and de Forster*, 1999]. It is important to describe the three-dimensional distribution and its temporal variation of ozone on a global basis in order to understand the atmospheric variability and climate change [*WMO*, 2011].

[3] Satellite observations of ozone have provided abundant information, especially about the global distribution of column ozone [e.g., *Stolarski and Frith*, 2006]. Vertical

[1]Research Institute for Global Change (RIGC), Japan Agency for Marine-Earth Science and Technology (JAMSTEC), Yokosuka, Japan.
[2]Graduate School of Science, Kobe University, Kobe, Japan.
[3]Faculty of Environmental Earth Science, Hokkaido University, Sapporo, Japan.
[4]Research Institute for Sustainable Humanosphere, Kyoto University, Uji, Kyoto, Japan.
[5]Department of Geography, Tokyo Metropolitan University, Hachioji, Japan.
[6]Aero-Meteorological Observatory, National Hydrometeorological Service, Ministry of Natural Resources and Environment, Hanoi, S. R. Vietnam.

Corresponding author: S-.Y. Ogino, Research Institute for Global Change (RIGC), Japan Agency for Marine-Earth Science and Technology (JAMSTEC), 2-15, Natsushima-cho, Yokosuka 237-0061, Japan. (ogino-sy@jamstec.go.jp)

©2013. American Geophysical Union. All Rights Reserved.
2169-897X/13/10.1002/jgrd.50348

profiles are observed with the nadia [e.g., *Hoogen et al*., 1999; *Kroon et al*., 2011] and limb [e.g., *Shiotani and Hasebe*, 1994; *Mieruch et al*., 2012] measurement techniques which have depicted the three-dimensional ozone distributions and their variabilities mainly in the middle atmosphere. Although tropospheric ozone profiles are now available by nadir sounding [e.g., *Worden et al*., 2007], they still have limitations in the vertical resolution and coverage. Therefore, balloon-borne ozonesondes remain a necessary tool for ozone observation. These ozonesondes have advantages in vertical resolution and wide vertical coverage through the troposphere and the lower stratosphere (surface to ∼30 km), even though an individual ozonesonde observation does not provide information about the horizontal variation.

[4] Ozonesonde observations operationally conducted by the meteorological agencies have a long time and global coverage. Most of the operational ozonesonde data are archived at World Ozone and Ultraviolet Radiation Data Centre (WOUDC) (http://www.woudc.org/). Since the operational ozonesonde stations tend to be located over the northern midlatitudes, the Southern Hemisphere Additional Ozonesondes (SHADOZ) recently established equatorial and southern hemispheric ozonesonde stations [*Thompson et al*., 2003a, 2003b, 2007, 2012]. However, there was no ozonesonde station before September 2004 that provided continuous data over the Indochina Peninsula, which is located at the southeastern edge of the Eurasian Continent.

[5] Since September 2004, we have conducted once or twice monthly regular ozonesonde observations in Hanoi (21.02°N, 105.80°E) at the base of the Indochina Peninsula. In addition, we have conducted campaign observations with ozonesondes and two types of water vapor sondes, Snow White [*Fujiwara et al.*, 2003a] and Cryogenic Frost point Hygrometer (CFH) [*Vömel et al*., 2007], seven times during every northern winter from 2004/2005 to 2010/2011 [e.g., *Fujiwara et al*., 2010]. In each campaign observation, ozone and water vapor sondes were launched at intervals of a few days during a 2–4 week period. Such continuous ozonesonde observation in this latitude region is rare on a global basis except for the operational observation at Hong Kong (22.31°N, 114.17°E) near Hanoi since 2000, where the obtained data are archived at the WOUDC. In this paper, the data at Hong Kong are also used as a reference. Hanoi has been one of the SHADOZ stations since 2010 [*Thompson et al*., 2012].

[6] Hanoi is located near the boundary between the tropical troposphere and extratropical stratosphere in the upper troposphere and lower stratosphere (UTLS) region, which is one of the important regions for the stratosphere-troposphere exchange (STE) [*Holton et al.*, 1995]. Hanoi is also located at the southeastern edge of the Asian monsoon circulation. The Asian monsoon is one of the most important circulations for the mass and energy exchanges between the tropics and the extratropics in the UTLS region [*Dunkerton*, 1995]. In the meaning mentioned above, the physical and chemical observations at Hanoi are expected to provide valuable information on the STE and the tropical-extratropical exchange. The purpose of this paper is to describe the basic variations in ozone and related meteorological parameters obtained at Hanoi, the newly established ozonesonde station. From the viewpoint of zonal mean atmospheric structure, it is expected that the seasonal variation in ozone in the subtropical UTLS region shows larger (smaller) values in winter (summer) because the boundary between the midlatitude LS and the tropical UT moves southward (northward) in winter (summer) and the air mass with high (low) ozone concentration in the midlatitude LS (the tropical UT) tends to be observed. However, it will be shown that the seasonal ozone variation at Hanoi is opposite to the one expected from the zonal mean viewpoint and is strongly affected by the zonally asymmetric atmospheric structure due to the Asian monsoon.

[7] In this paper, we describe the seasonal and subseasonal variations in the ozone mixing ratio (OMR) revealed by the ozonesonde observations at Hanoi. In section 2, we describe the details of ozonesonde observations conducted at Hanoi, the other data used for comparison, and the analysis method. The characteristics of seasonal variations and subseasonal variations in ozone are shown in section 3. The source of the variations is discussed by comparing with the meteorological fields and the global ozone distributions. Section 4 summarizes the results of the description and the discussion.

2. Observation and Data

2.1. Ozonesonde Observation at Hanoi

[8] We started regular ozonesonde observations in September 2004 at the Aero-Meteorological Observatory in Hanoi (21.02°N, 105.80°E; WMO station number: 48820), Vietnam. We have conducted once-monthly ozonesonde observations since then. The launch frequency was increased to twice monthly during the period from February 2006 to October 2010.

[9] Seven intensive campaign observations with ozone and water vapor sondes have been conducted in every northern winter (December 2004/January 2005, January 2006, January 2007, January 2008, January 2009, January 2010, and January 2011) under the Soundings of Ozone and Water in the Equatorial Region (SOWER) project [e.g., *Fujiwara et al*., 2010]. During each campaign period (2–4 weeks), we launched ozone and water vapor sondes every few days. The number of intensive ozonesonde launches for each campaign is as follows: 8 in the first campaign (December 2004 to January 2005), 16 in the second (January 2006), 6 in the third (January 2007), 5 in the fourth (January 2008), 4 in the fifth (January 2009), 5 in the sixth (January 2010), and 3 in the seventh (January 2011). We use these campaign data to describe the subseasonal and day-to-day variabilities in ozone during the wintertime.

[10] The monthly observations were conducted by using a set of an ozonesonde and a radiosonde to obtain the ozone concentration, pressure, temperature, and humidity data from the surface up to about 30 km. Three types of ozonesonde-radiosonde combinations were used. Depending on the combinations, different types of sensor solutions were used. During the period from September 2004 to April 2009, a combination of an Ensci 1Z ECC ozonesonde and a Vaisala RS80 radiosonde without a wind finding module were used with a 2%-KI unbuffered solution (combination 1). A Science Pump Corporation ECC-6A ozonesonde and a Vaisala RS92-SGP radiosonde with a 1%-KI buffered solution (combination 2) were used during the period from May 2009 to June 2010. An Ensci Model-Z ECC ozonesonde and

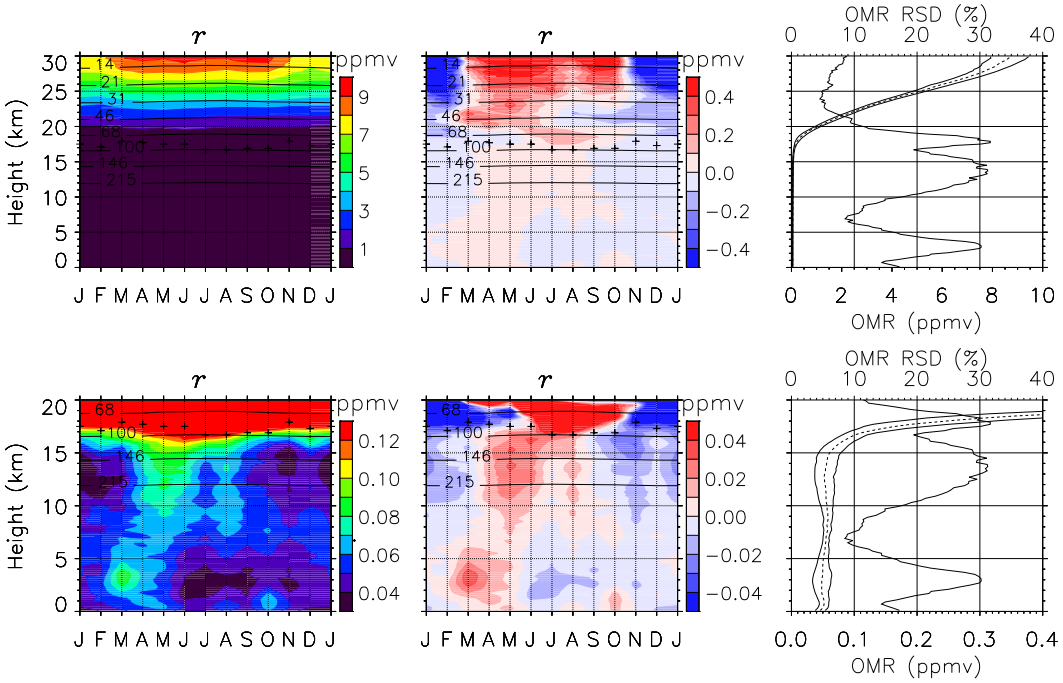


Figure 1. (left) Mean seasonal variation of OMR obtained by calculating monthly mean values at each height and at each month from September 2004 to November 2011. (center) Same as the left panels but showing the OMR anomalies from the annual mean at each height. (right) Vertical profiles of annual mean OMR (thick dashed line), standard deviation of OMR mean seasonal variation (thin solid line), and standard deviation normalized by the annual mean OMR at each height (thick solid line). Plus marks in left and center panels indicate cold point tropopauses determined by the long-term monthly mean temperature profiles. The upper panels show the height range of 0–30 km, while the lower panels focus on the variations in the UTLS and the tropospheric regions from 0 to 20 km.

a Vaisala RS92-SGP radiosonde with a 0.5%-KI buffered solution (combination 3) have been used since July 2010. The wind data have been available since May 2009 for the observations launched with the RS92-SGP radiosonde.

[11] In laboratory intercomparisons, differences in ozone values measured by ECC ozonesondes with different instrument and solution types were shown by *Smit et al.* [2007]. According to their result, combinations 1, 2, and 3 used at Hanoi have biases relative to the reference measurement by the UV-photometer of at most –5%, +5%, and +5%, respectively. This means that the comparison between the ozonesonde data before and after the switch from combination 1 to combination 2 in May 2009 may have a relative bias of at most 10%. However, the present study does not contain such a comparison. In section 3.1, we investigate the 7 year mean seasonal variations. The biases do not affect the qualitative investigation of the mean seasonal variations, because the usage of instrument-solution combinations does not have any seasonal dependence. It is also noted that, since the data taken by the three types of combinations are mixed when we estimate the monthly mean values, the biases tend to be canceled out. The exception is the data of the winter campaigns in every January. Only combination 1, an Ensci 1Z ECC ozonesonde and a 2%-KI unbuffered solution, has been used for the campaign observations. Therefore, the monthly mean data in January may have a negative bias relative to other months. However, this bias is considered to be negligible in this paper, because we will examine the seasonal variability larger than 20–30%. This point will be mentioned again in section 3.1. In section 3.2, we investigate the subseasonal and day-to-day variabilities by using non-averaged data, in which the precision of the measurements with the fixed instrument and solution should be taken into account. According to the result by *Smit et al.* [2007], the precision for each sensor type and solution is less than 5%. That is much smaller than the variabilities discussed in section 3.2. Note that recently it is planned to homogenize the ozonesonde data sets from different types of solutions and sensors in an activity, "Ozone Sonde Data Quality Assessment (O3S-DQA)," as a part of SPARC-IGACO-IOC Initiative on "Past Changes in the Vertical Distribution of Ozone" (*Smit et al.,* 2012, Guide Lines for Homogenization of Ozone Sonde Data, http://www-das.uwyo.edu/~deshler/NDACC_O3Sondes/O3s_DQA/O3S-DQA-Guidelines%20Homogenization-V2-19November2012.doc).

[12] In this paper, we discuss the time variations of the OMR at various time scales at various height regions from the surface to the stratosphere. Because the OMR varies rapidly with height, it is reasonable to evaluate the amplitude of variation by quantities relative to the mean. Here, the amplitude is evaluated by the "relative standard deviation" (RSD). A RSD is defined as a standard deviation (SD) divided by a mean; the RSD is also called the "coefficient of variation" in general.

[13] In this paper, we also use the weekly ozonesonde data obtained at Hong Kong (22.31°N, 114.17°E) during 2000–2011 provided by WOUDC. The data were processed by the same methods as the Hanoi data and used as a reference.

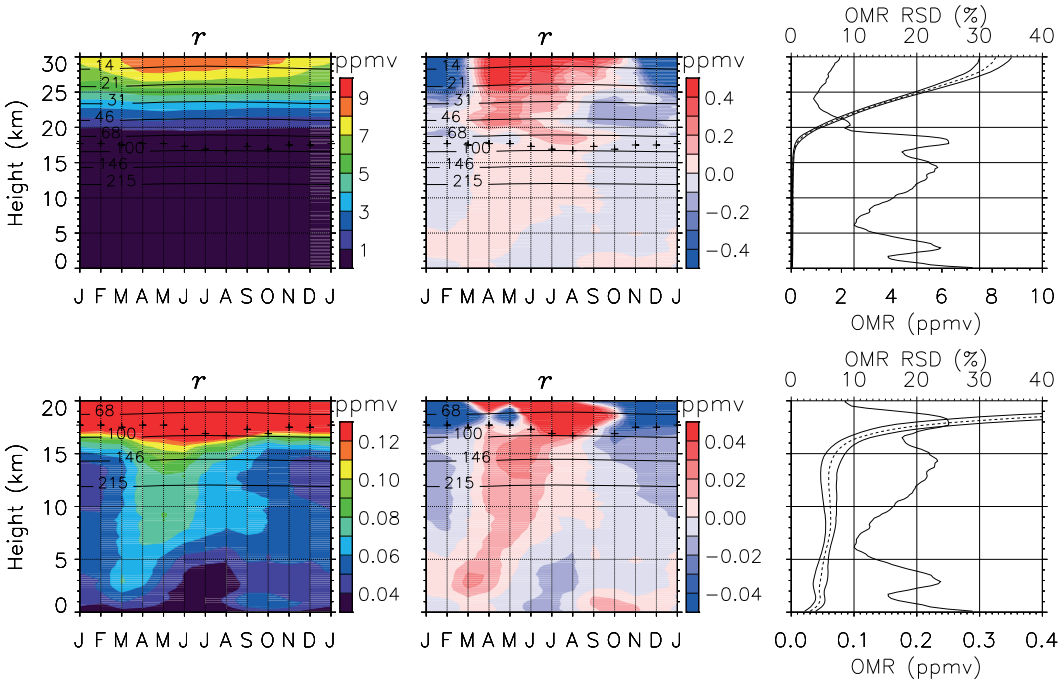


Figure 2. The same as Figure 1 except for the results obtained from the ozonesonde data at Hong Kong from 2000 to 2010.

2.2. Global Meteorological and Ozone Data

[14] To interpret the ozone variations observed at Hanoi, we also analyzed the global reanalysis and satellite ozone data. We used the National Centers for Environmental Prediction (NCEP) Reanalysis-II data [*Kanamitsu et al.*, 2002] with temporal interval of 6 h, horizontal resolution of 2.5×2.5°, and pressure levels of 1000, 925, 850, 700, 600, 500, 400, 300, 250, 200, 150, 100, 70, 50, 30, 20, and 10 hPa during 2004–2010 for analyzing the meteorological fields related to the ozone variations observed at Hanoi and to calculate isentropic backward trajectories.

[15] We also used the ozone profiles retrieved by the Aura/Microwave Limb Sounder (MLS) retrieval scheme version 2.2 Level 2 [*Livesey et al.*, 2006; *Jiang et al.*, 2007] to investigate the horizontal distributions of ozone. The Aura/MLS data were chosen because these resolve the vertical distribution, and the data period (from August 2004 to the present) just covers the ozonesonde observations at Hanoi. We exclude from our analysis the data below 215 hPa that is the lowest level of Aura/MLS ozone measurements. We removed the MLS data with erroneous values from our analysis in accordance with the recommendations in the data description document by the Jet Propulsion Laboratory [*Livesey et al.*, 2007]. The pressure levels used are 215.443 (the lowest level of the Aura/MLS ozone measurements), 146.780, 100.000, 68.1292, 46.4159, 31.6228, 21.5443, 14.6780, 10.0000, 6.81292, and 4.64159 hPa (very few ozonesonde data are available above this level). The climatological monthly means for the 8 years were obtained from the monthly mean data gridded on to 5° × 5° bins.

[16] In addition, we used the monthly mean outgoing long-wave radiation (OLR) provided by the National Oceanic and Atmospheric Administration (NOAA) [*Liebmann and Smith*, 1996] with a horizontal resolution of 2.5° longitude × 2.5° latitude from 2004 to 2010 to compare the ozone variations with the convective activities.

3. Results and Discussion

3.1. Seasonal Variations

[17] Figure 1 shows the mean seasonal variations of OMR at Hanoi (left panels). The long-term monthly mean values since September 2004 are used for this plot. The OMR anomaly from the annual mean is also shown in the center panels. The means, the SDs, and the RSDs (the SDs normalized by the annual mean) are plotted in the right panels of Figure 1. The similar plots obtained by the data at Hong Kong are shown in Figure 2. The results showed quite similar seasonal variations at both stations, suggesting that the data are reliable and the obtained variations are robust. The characteristics of the mean seasonal variation seen at both stations are described below.

[18] In the lower and middle stratosphere (above about 20 km height, shown in the upper panels of Figure 1), a clear seasonal variation is found with larger values in spring and summer and with smaller values in winter. The mean value and the SD rapidly increase with height, while the RSD ranges by 5%–10% through this height range. Since the normal SD tends to increase for the variable with large mean value, the RSD is more appropriate for the evaluation of variables of which mean value rapidly changes. The seasonal variation with the spring-summer maximum is consistent with the well-known features of seasonal variation in the ozone shown by *Shiotani and Hasebe* [1994] using satellite ozone data. This reflects the seasonality of both the Brewer-Dobson circulation and the photochemical production. This aspect of seasonality will not be discussed further.

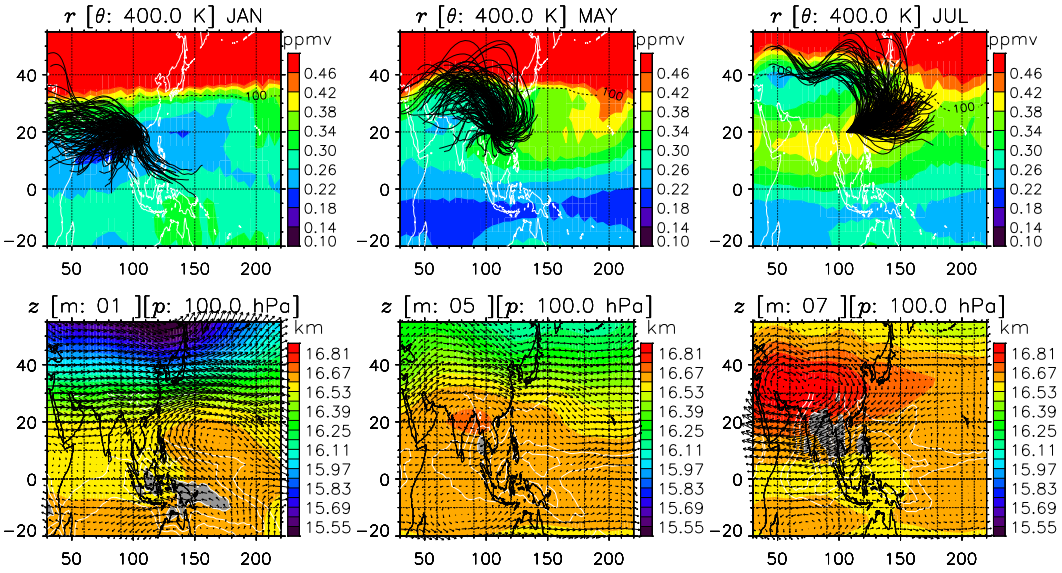


Figure 3. Upper panels show 5 day backward trajectories starting at every 06:00 UT (13:00 LT in Vietnam) the Aura/MLS OMR (color shades) and the NCEP Reanalysis pressure (broken contours) in (left) January, (center) May, and (right) July at 400 K surface (at about 18 km over Hanoi). Lower panels show climatological monthly mean geopotential height (color shade), horizontal wind (arrow), and OLR (contour and gray shade) in (left) January, (center) May, and (right) July at 100 hPa (about 400 K near Hanoi). Contour levels for OLR are 180, 200, 220, and 240 W/m^2. The areas below 180 and 200 W/m^2 are shaded by dark and light gray colors, respectively. Note that OLR contours in the area north of 30°N are not displayed, because they are possibly contaminated by the cold land surface.

[19] A clear seasonal cycle with a winter minimum is also found in the upper troposphere and lower stratosphere (UTLS) region (10–20 km shown in the lower panels of Figure 1) with the RSD of 20–30%. In more detail, the RSD has double peaks in height at about 14 km and about 18 km. The seasonal variability appears to be different above and below the cold point tropopause (indicated by the plus marks in Figure 1) at around 17 km height. Below the tropopause level (upper troposphere near 14 km), the OMR peaks in late spring (May), while above it (lower stratosphere near 18 km) the OMR peaks in summer (July to August). It is possible that the processes resulting in these variations are different. This point is discussed below in terms of the air mass transport. It should be noted that the winter minimum in January should be considered carefully because the data in January may have a negative bias as mentioned in section 2. It is confirmed that the data at the Hong Kong station in Figure 2 show the similar minimum in January.

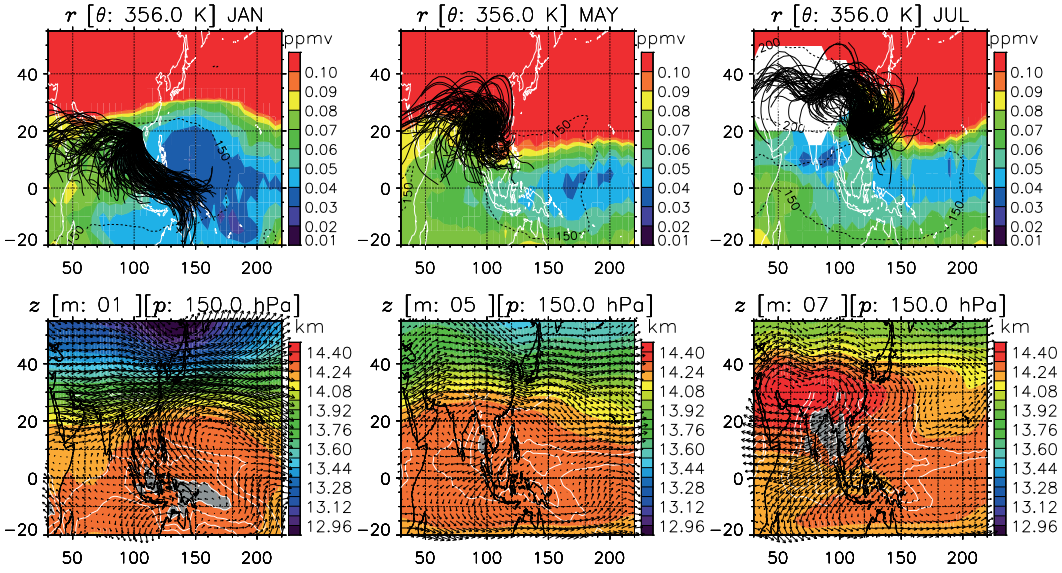


Figure 4. The same as Figure 3 but (upper) at 356 K surface (at about 14 km over Hanoi) and (lower) at 150 hPa (about 356 K near Hanoi).

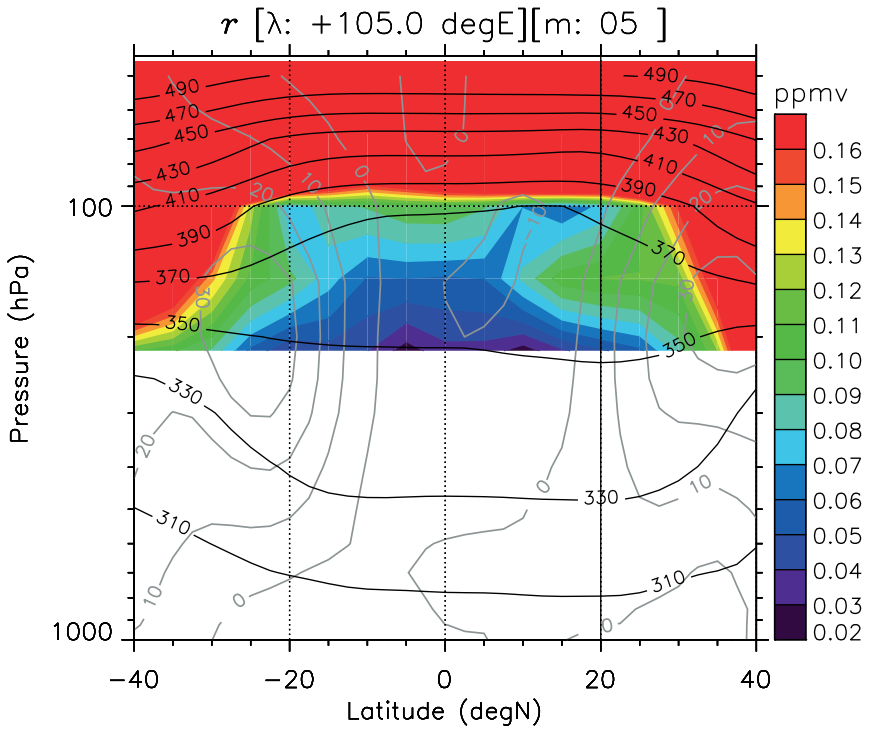


Figure 5. Latitude-pressure section of climatological mean Aura/MLS OMR in May along 105°E. Black contours show the NCEP Reanalysis isentropes, and gray contours show the NCEP Reanalysis zonal wind.

Therefore, it is said that the minimum in January may not be caused only by the expected negative bias but reflects the nature.

[20] The upper panels of Figure 3 show 5 day backward trajectories starting from Hanoi at every 06:00 UT (13:00 LT in Vietnam) in winter (January), late spring (May), and summer (July) for all years at the 400 K isentropic surface (about 18 km height over Hanoi) and at the 356 K surface (about 14 km height over Hanoi). The backward trajectories were calculated every 30 min on isentropic surfaces by using the linearly interpolated NCEP reanalysis data and by the second-order Runge-Kutta method for time integration, as done previously by *Fujiwara et al.* [2003b] and *Hasebe et al.* [2007]. The monthly mean background OMRs obtained by Aura/MLS during 2004–2010 are also plotted in the upper panels of Figure 3. Corresponding meteorological fields, the geopotential height, horizontal winds, and OLR are shown in the lower panels of Figure 3, and the same plots for upper troposphere (around 14 km height near Hanoi) are shown in Figure 4. Note that the white color region over and around the Tibetan Plateau (30°E–100°E, 20°N–50°N) in the panel for July at 356 K indicates that the Aura/MLS OMR data are not available because the level is below the lower limit (215 hPa) of the Aura/MLS ozone observation [*Livesey et al.*, 2007], which is due to the Tibetan High development over the region as seen in the lower right panel of Figure 4. In the following, the overall features of trajectories in each month are compared with the climatological mean of the Aura/MLS OMR and the meteorological fields.

[21] In winter, air masses are transported from the equatorial and subtropical upper troposphere over the Maritime Continent, the Indian Ocean, South Asia, and West Africa where the mean OMRs are smaller than those in the midlatitude and high-latitude regions. This feature is commonly seen through the UTLS region in winter. The anticyclonic circulation formed over the northern part of the western Pacific in winter (lower left panels of Figures 3 and 4) is considered to be a Rossby response to the convective heating over the Maritime Continent and the equatorial western Pacific region [*Highwood and Hoskins*, 1998; *Hatsushika and Yamazaki*, 2003]. It is assumed that this type of horizontal transport is the cause of the OMR minimum in winter UTLS region over Hanoi.

[22] In late spring (May), convective center moves northwestward, and the associated monsoon high and anticyclonic circulation begin to develop in the UTLS region over and around the Bay of Bengal as seen in the lower middle panels of Figures 3 and 4. As seen in Figure 1, the upper tropospheric OMR over Hanoi increases in May at the height range from 10 to 16 km. This increase is consistent with the cross-tropopause, isentropic air mass transport from the midlatitude stratosphere possibly due to the Rossby wave breaking, which is known to occur frequently in late spring at around the 350 K surface [e.g., *Appenzelle et al.*, 1996; *Seo and Bowman*, 2001]. We emphasize that the location of Hanoi is appropriate for the observation of the cross-tropopause mass exchange in this season. In summer (July), the region of high ozone concentration at the 356 K surface moves to the Pacific region, as seen in the lower right panel of Figure 4, and the OMR around Hanoi decreases. This move is consistent with the results by *Postel and Hitchman* [1999], who showed that the Rossby wave breaking occurs most actively in the Pacific region in the northern summer.

[23] At the 400 K surface, a similar anticyclonic flow seems to transport the midlatitude air to the tropics (lower

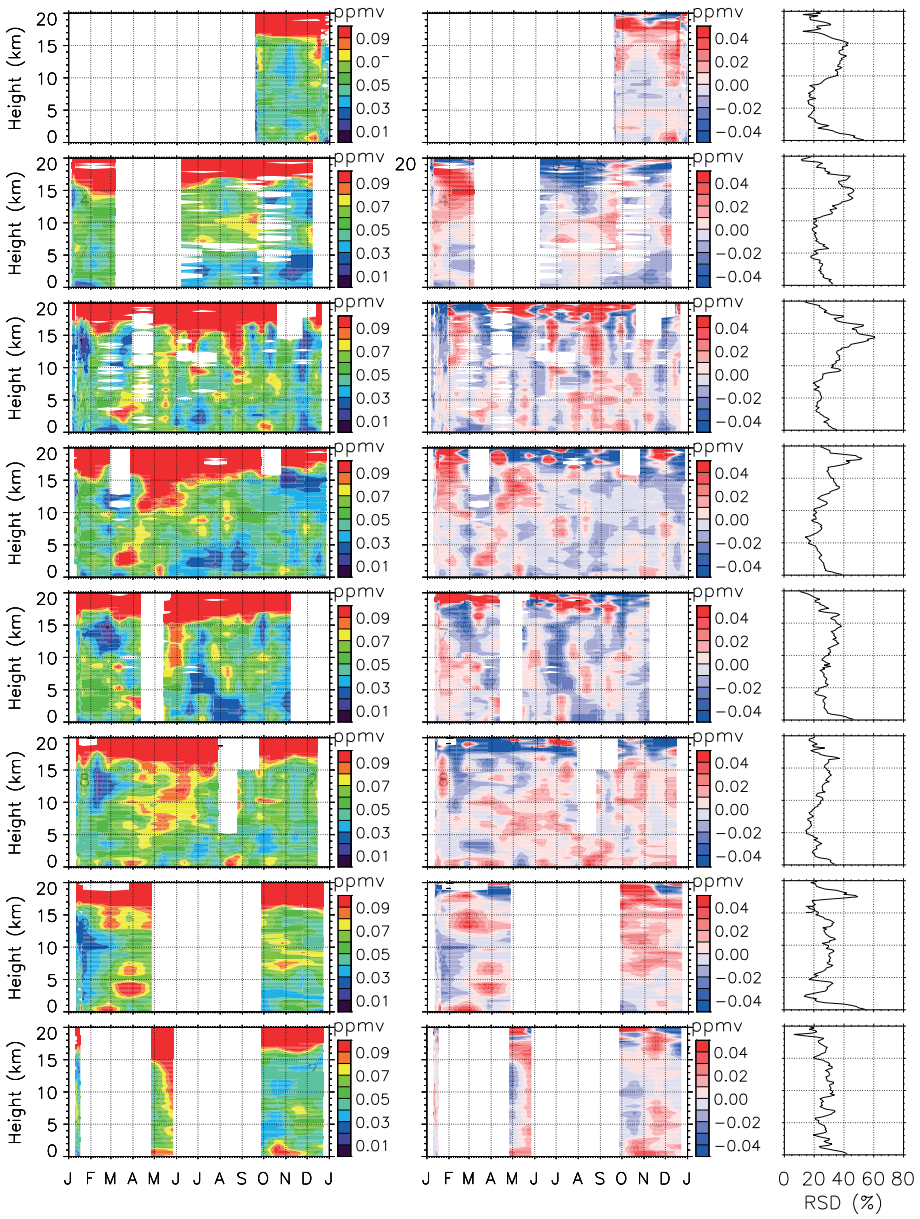


Figure 6. Time height sections of (left) OMR, (center) OMR anomaly from the mean seasonal variation, and (right) vertical profiles of the RSD (the SD of the OMR anomaly from the mean seasonal variation normalized by the annual mean of each year) from (top) 2004 to (bottom) 2011.

right panel of Figure 3). However, the OMR distribution (upper right panel of Figure 3) formed by the anticyclonic circulation is somewhat different from that in the upper troposphere. As seen in the upper center and right panels of Figure 4, the horizontal OMR distribution in the lower stratosphere has a coherent tongue-shaped structure extending from the central Pacific to the Indian Ocean with a horizontal scale of ∼1000 km or larger. It should also be noted that this tongue-shaped structure is vertically separated from the upper tropospheric ozone increase, as shown in Figure 5. In Figure 5, a high OMR intrusion is seen from the midlatitude stratosphere at a latitude of 20°N–30°N near the 360K surface, while apart from the intrusion, an OMR increase is seen near 10°N at around the 380 K surface, which is due to the tongue-shaped OMR transport from the midlatitude stratosphere. The lower stratospheric increase seems to be caused directly by the anticyclonic circulation associated with the Tibetan High, which is different from the upper tropospheric increase possibly due to the Rossby wave breakings. This feature is consistent with the results of chemical transport model and the data analyses shown by *Konopka et al.* [2010]. The anticyclonic circulation in the lower stratosphere appears in late spring and develops until midsummer as a thermodynamical response of Asian monsoon convective activity [*Randel and Park*, 2006; *Park et al.*, 2007]. In July–August, a well-developed tongue-shaped structure with high OMR air masses moves over Hanoi. As a result, the maximum OMR is considered to appear at around 18 km height in summer over Hanoi.

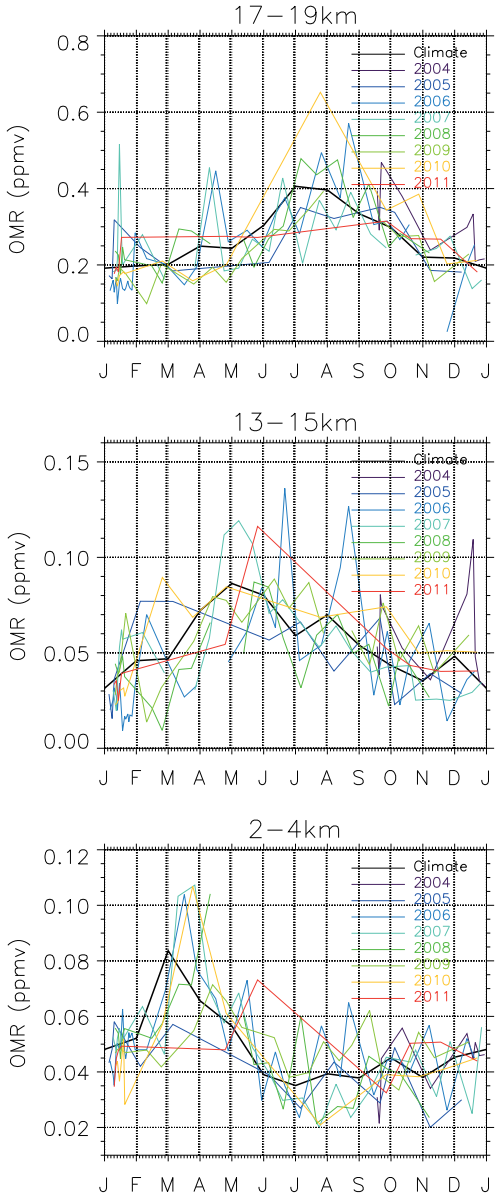


Figure 7. Temporal variations of the OMR averaged at (bottom) 2–4 km, (center) 13–15 km, and (top) 17–19 km bins in each year from 2004 to 2011. The climatological seasonal variation is also plotted with black line.

[24] Hanoi is located at the northwestern edge and at the southeastern edge of the anticyclonic circulation due to the Rossby response in winter and in summer, respectively. Therefore, it is concluded that the seasonal variation in the UTLS ozone observed at Hanoi is caused by the seasonal change in the source of the air mass associated with the large-scale, monsoon-related circulation change, although the detailed behaviors are different between the height ranges above and below the tropopause.

[25] In the middle troposphere (5–10 km), the seasonal variability of OMR is small with the relative standard deviation of 10%–20% as seen in Figure 1. The weak maxima are seen in late spring (May), summer (August), and autumn (October).

[26] In the lower troposphere, the OMR has a clear maximum in March to April at about 3 km height. It is known that surface ozone enhancement occurs in this season in the East and Southeast Asian regions [e.g., *Pochanart et al.*, 2001; *Tanimoto et al.*, 2005]. *Pochanart et al.* [2001] indicated that the spring maximum of the surface ozone over Thailand was caused by the ozone production due to biomass burning in Southeast Asia. Indeed, it is clearly seen that the near-surface ozone increases during the same months. It is possible that the ozone increase at about 3 km height is related with the surface ozone enhancement due to the biomass burning through vertical diffusion or transport. It is known that strong temperature inversions frequently develop over the Indochina Peninsula in spring [*Nodzu et al.*, 2006; *Ogino et al.*, 2010; *Nodzu et al.*, 2011]. *Nodzu et al.* [2006] showed that the temperature inversions typically appear at two levels, about 1.5 km and about 4 km in March to April over Hanoi. It is interesting that the OMR maximum observed with the ozonesondes appears between the heights of these double inversions. This relationship implies that the double layered structure of atmospheric stability plays a role in determining the vertical transport or accumulation process of high OMR air masses over the Indochina Peninsula.

[27] Deep intrusions of the stratospheric air into the troposphere associated with tropopause foldings [e.g., *Elbern et al.*, 1997; *Stohl et al.*, 2003] are another candidate for producing the spring ozone maximum at 3 km. This ozone maximum also seems to have a source from the upper tropospheric ozone increase in May discussed above. The warm air intrusion from the stratosphere due to the tropopause folding must produce a steep temperature change within the troposphere, which is consistent with the coexistence of temperature inversions and ozone maximum.

[28] The results and discussions above suggest that the consideration of three-dimensional transport is important for understanding the spring increase in ozone at 3 km. Further studies, such as three-dimensional trajectory analysis and numerical experiments using a chemical transport model, are expected to clarify the generation mechanism of the ozone maximum in spring.

[29] An ozone enhancement near the surface in October is also clearly seen in Figure 1, as also seen in Figure 3 of the paper by *Thompson et al.* [2012]. The same feature is found in the result at Hong Kong (Figure 2). Biomass burning is not active in October over the southeast Asian region [e.g., *Duncan et al.*, 2003], which is different from the spring case mentioned above. Therefore, we should consider the cause of this enhancement other than the pollution due to biomass burning. Further studies would be expected to clarify it.

3.2. Subseasonal Variations

[30] Next, we investigate the subseasonal variations in OMR observed by the ozonesondes at Hanoi. Figure 6 shows the OMR variations for every year from 2004 to 2011. The left panels show the OMR measured values. The center panels show the OMR anomalies from the 8 year mean seasonal variation, i.e., deseasonalized OMR variations. The right panels show vertical profiles of the RSD of the deseasonalized OMR variations. Both the data from the monthly and the intensive campaign observations were used for these figures. From the left and center panels, we find the

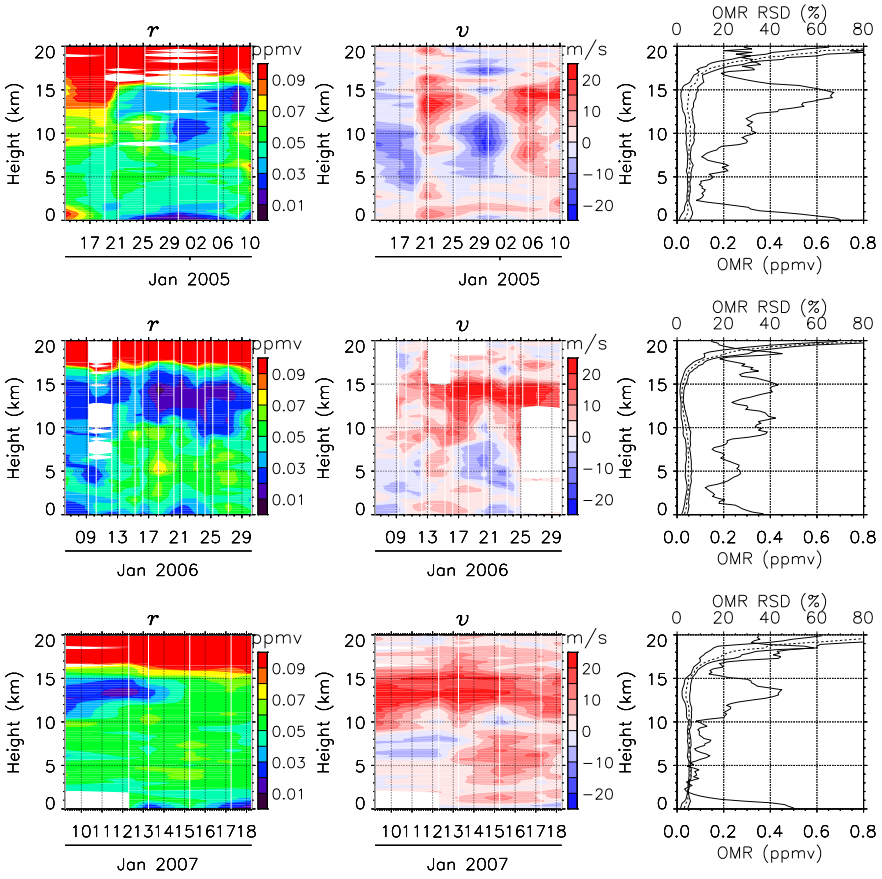


Figure 8. Time height sections of (left) OMR and (center) meridional wind, and (right) vertical profiles of statistical values of OMR: (thick dashed line) campaign-mean OMR, (thin solid line) standard deviation, and (thick solid line) relative standard deviation for (top) the first (December 2004 and January 2005), (middle) the second (January 2006), and (bottom) the third (January 2007) campaign observations. Vertical white lines in the time height sections denote the launch time of the ozonesonde.

subseasonal variations have a significant magnitude in addition to the mean seasonal variability.

[31] These features are more clearly seen from the line plots at selected heights shown in Figure 7. We can recognize the characteristics of the mean seasonal variation of the OMR with the lower tropospheric (2–4 km) early spring (March–April) maximum, the upper tropospheric (13–15 km) late spring (May–June) maximum, and the lower stratospheric (17–19 km) summer (July–August) maximum in almost all years. In addition to such a clear seasonal cycle, the subseasonal variation of the OMR is also dominant through the year.

[32] The RSD for each year is shown in the right panel of Figure 6. It is seen that the RSDs have larger values in the UTLS region near 15 km height as a common feature for every year except for years 2010 and 2011. Their values are around 40%, which is comparable to that of the mean seasonal variation at the same height region. Note that the exception for years 2010 and 2011 is considered partly because of the gap in the data. The RSDs in the boundary layer (below 1 km height) are also large.

[33] The monthly ozonesonde observations at Hanoi have been conducted once or twice per month, and their sampling interval is not constant. Therefore, it is difficult to investigate the dominant phenomena only from this data set. However, we have conducted campaign ozonesonde observations at intervals of a few days during every winter. Here, we examine the campaign observation data to investigate the ozone variations at a time scale of a few to several days.

[34] Examples of OMR variations during the first, second, and third campaigns are shown in Figure 8. The layered OMR minima with a vertical scale of 2–3 km in the UTLS region near the 15 km height are clearly seen for all the three campaign observations. For example, in the first campaign

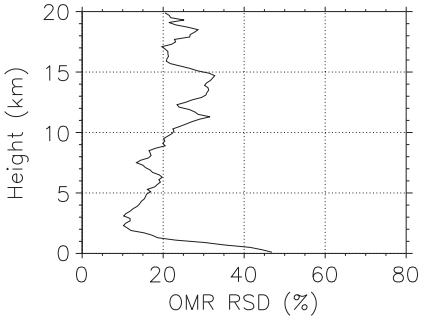


Figure 9. Vertical profile of mean OMR relative standard deviation for the results of all campaign observations.

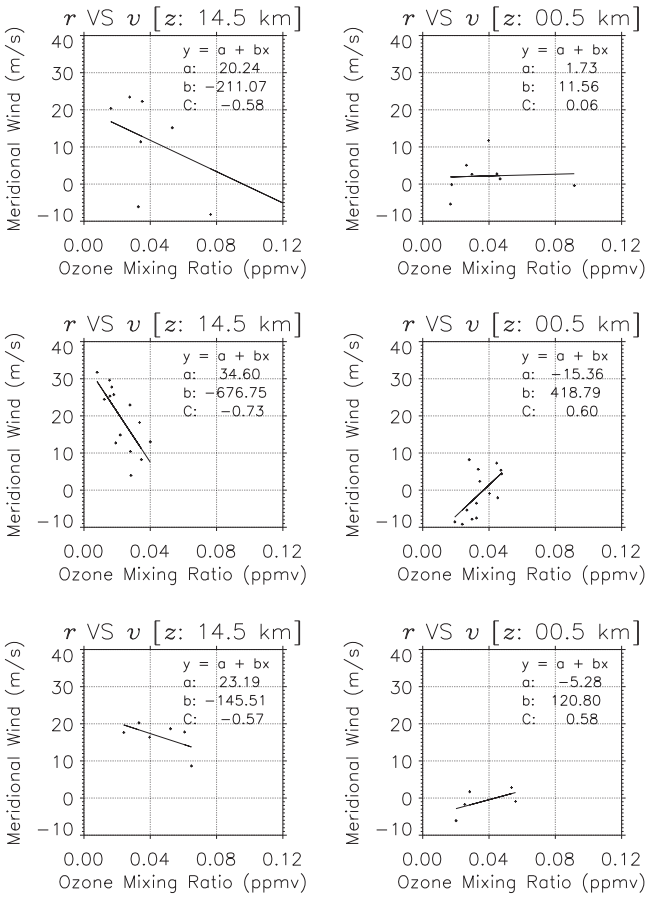


Figure 10. Scatter plots of OMR versus meridional wind averaged at height ranges of (left) 14–15 km and (right) 0–1 km for (top) the first (December 2004 and January 2005), (middle) the second (January 2006), and (bottom) the third (January 2007) campaign observations.

period, an OMR minimum appears near the 14 km height during 4–8 January. Similar OMR minima are found during 17–29 January 2006 at around 14 km and during 10–14 January 2007 at around 13 km. Vertical profiles of OMR RSDs are shown in the right panels in Figure 8. In this figure, the large variability of ozone in the UTLS is found with the RSD of 40%–60% near the 14 km height. The similar feature (maximum RSD of about 30% in the UTLS region) is found in the mean RSD profile for all the results from the seven campaigns in every winter (Figure 9). It is also seen that the near-surface variations have large amplitudes with the RSD of 40%–70%.

[35] The variation in the UTLS region seems to have a close relation with the background meridional wind as shown in the center panels of Figure 8. This relation is examined in more detail below, since it supports the result of the backward trajectory analyses shown in section 3.1 that the OMR value observed at Hanoi has a dependency on the air mass origin. The strong northward wind in the UTLS region coincides with the OMR minima described above. The scatter plots show a negative correlation between the OMR and the meridional wind variations averaged over 14–15 km height range as shown in the left panels in Figure 10. The correlation coefficient is estimated as approximately –0.6 as the mean value of the three campaign data. It is also found that the OMR has a positive correlation with the zonal wind with the correlation coefficient of approximately +0.8 (not shown). These results indicate that the eastward-oriented (weak northward and strong eastward) wind tends to transport low OMR air masses and the northward-oriented (strong northward and weak eastward) wind tends to transport high OMR air masses to Hanoi. In the boundary layer, a positive correlation between the OMR

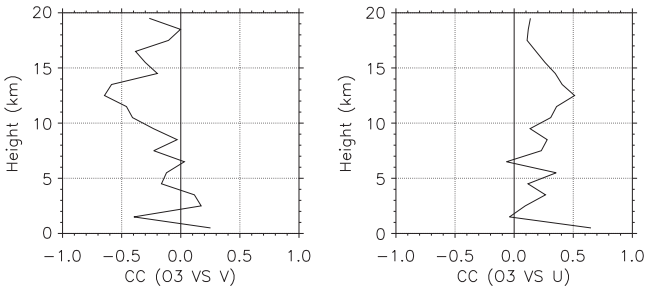


Figure 11. Vertical profiles of correlation coefficient between the OMR and the meridional wind (left panel) and between the OMR and the zonal wind (right panel) at every 1 km bin from the surface up to 20 km. The correlation coefficient is the averaged value for the results of all campaign observations.

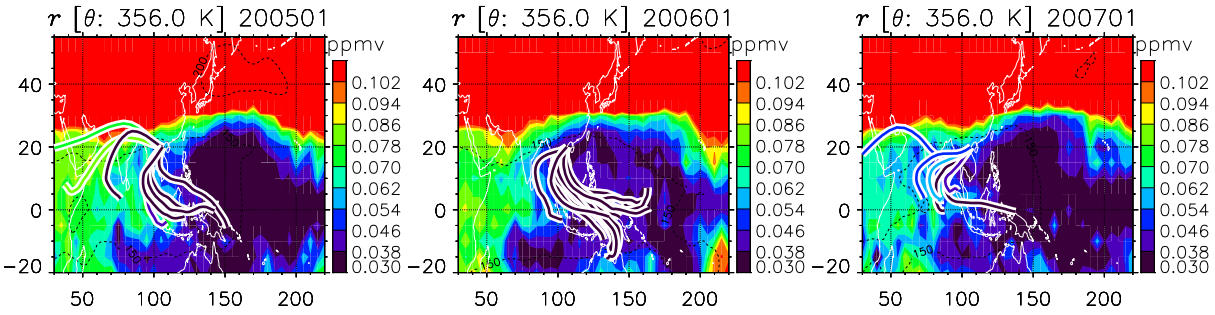


Figure 12. Backward trajectories at 356 K surface starting at the time of campaign ozonesonde launches for (left) December 2004 and January 2005, (center) January 2006, and (right) January 2007. Monthly mean Aura/MLS OMR is shaded by color. Lines and shades share the same colors showing the values of ozone mixing ratio.

and the meridional wind is found with a correlation coefficient of approximately 0.4 as the mean value of the three campaign data.

[36] Figure 11 shows vertical profiles of the correlation coefficient between the OMR and the meridional wind (left panel) and between the OMR and the zonal wind (right panel) at every 1 km bin from the surface to 20 km. The correlation coefficient is the average of all results from the seven wintertime campaign observations. It is found that the negative (positive) correlation between the OMR and the meridional (zonal) wind in the UTLS region is a prominent feature. The student's t test for the null correlation between OMR and meridional wind in UTLS in January 2006, when we conducted 14 soundings that were the largest number among the all winter campaigns, showed that the negative correlation is statistically significant at the 95% level. Based on these facts, we consider that the correlations between OMR and the horizontal winds are the significant feature in the UTLS region at Hanoi. In the boundary layer, on the other hand, the positive correlation between the OMR and the meridional wind does not seem to be robust, although the large amplitude and the positive correlation are seen in the first three campaign observations.

[37] In the left panels of Figure 12, backward trajectories on the 356 K surface starting at Hanoi at the launch time of the first, second, and third campaign ozonesonde observations are plotted with colors indicating the observed OMR values. These trajectories show that the lower (higher) OMR values tend to be traced back to the Maritime Continents and the western Pacific (to the Indian Ocean and African region). This result is consistent with the negative correlation between the OMR and the meridional wind in the UTLS region over Hanoi and supports the interpretation that the OMR winter minimum in the UTLS is caused by the low OMR air mass transport from the equatorial region where the mean ozone concentration is low.

4. Summary

[38] We have conducted continuous monthly ozonesonde observations and intensive campaign observations with intervals of a few days for every winter at Hanoi (21.02°N, 105.80°E), Vietnam since September 2004. By using the obtained data, seasonal and subseasonal variations in the ozone mixing ratio (OMR) are investigated, and the causes of the variations are discussed. The relative standard deviation (RSD), which is defined as the standard deviation normalized by the mean value, is employed to evaluate the amplitude of variation to eliminate the rapid increase of the mean OMR with height.

[39] In the lower and middle stratosphere (above about 20 km height), a clear seasonal variation is found with larger values in spring and summer and with smaller values in winter. This result is consistent with the well-known features of seasonal variation shown in previous studies [*Shiotani and Hasebe*, 1994].

[40] A seasonal cycle with a winter minimum and a spring-summer maximum is also found in the UTLS region (10–20 km) with larger RSD of 20%–30%. A backward trajectory analysis shows that the winter minimum is due to the low OMR air mass transport from the tropical troposphere. This feature is commonly seen through the UTLS region in winter. In contrast, the variation from spring to summer seems to be different above and below the tropopause level at around 17 km. Below the tropopause level (upper troposphere near 14 km), the OMR peaks in late spring (May). This peak is consistent with the air mass transport from the midlatitude stratosphere to the troposphere possibly due to Rossby wave breakings. Above the tropopause level (lower stratosphere near 18 km), the OMR peaks in summer (July to August). This peak seems to be caused directly by the anticyclonic circulation associated with the Tibetan High, which is different from the upper tropospheric increase. In midsummer, the well-developed tongue-shaped structure with high OMR air masses moves over Hanoi. As a result, the maximum OMR is considered to appear at around 18 km height in summer over Hanoi.

[41] In the lower troposphere, the OMR has a clear maximum in March to April at about 3 km height. The maximum seems to propagate downward from 3 km height to the surface ozone maximum in May. The relation with surface ozone enhancement due to biomass burning is suggested. Tropopause folding is another candidate for producing the spring ozone maximum at 3 km.

[42] Subseasonal variations in the OMR show large amplitudes in the UTLS region (around 15 km) and in the boundary layer (below 1 km) with the RSD larger than 40%, which is comparable to those of mean seasonal variation of the OMR. It is shown that the OMR variation in the UTLS region during every winter campaign has a negative

correlation with the meridional wind. This relation indicates that the low OMR air masses observed at Hanoi have been transported from the equatorial region, which is confirmed by the backward trajectory analyses. These results support the interpretation that the OMR winter minimum in the UTLS is caused by the low OMR air mass transport from the equatorial region, where the mean ozone concentration is low.

[43] **Acknowledgments.** The authors thank the staff at the Aero-Meteorological Observatory, Hanoi, National Hydrometeorological Service of Vietnam for their help in obtaining the valuable ozonesonde data. The present work was partly supported by Grants-in-Aid for Scientific Research (A) No. 15204043 and (A) No. 18204041, the Ministry of Education, Culture, Sports, Science and Technology, by the Global Environment Research Fund (A-071), the Ministry of the Environment, and by Kyoto University Active Geosphere Investigations for the 21st Century Centers of Excellence (COE) Program. Some of the ozonesondes were provided by the National Oceanic and Atmospheric Administration (NOAA) and the National Aeronautics and Space Administration (NASA). The trajectory model used in this study was developed at the Earth Observation Research Center (EORC), National Space and Development Agency (NASDA) (now Japan Aerospace Exploration Agency, JAXA).

References

Appenzelle, C., J. R. Holton, and K. H. Rosenlof (1996), Seasonal variation of mass transport across the tropopause, *J. Geophys. Res.*, *101*(D10), 15,071–15,078.

Brasseur, G. P., R. G. Prinn, and A. A. Pszenny (eds.) (2003), *Atmospheric Chemistry in a Changing World*, 300 pp., Springer-Verlag, Berlin.

Duncan, B. N., R. V. Martin, A. C. Staudt, R. Yevich, and J. A. Logan (2003), Interannual and seasonal variability of biomass burning constrained by satellite observations, *J. Geophys. Res.*, *108*(D2), 4100, doi: 10.1029/2002JD002378.

Dunkerton, T. J. (1995), Evidence of meridional motion in the summer lower stratosphere adjacent to monsoon regions, *J. Geophys. Res.*, *100*, 16,675–16,688.

Elbern, H., J. Kowol, R. Sládkovic, and A. Ebel (1997), Deep stratospheric intrusions: A statistical assessment with model guided analyses, *Atmos. Environ.*, *31*(19), 3207–3226, doi:10.1016/S1352-2310(97)00063-0.

Fujiwara, M., M. Shiotani, F. Hasebe, H. Vömel, S. J. Oltmans, P. Ruppert, T. Horinouchi, and T. Tsuda (2003a), Performance of the Meteolabor "Snow White" chilled-mirror hygrometer in the tropical troposphere: Comparisons with the Vaisala RS80 A/H-Humicap sensors, *J. Atmos. Oceanic Technol.*, *20*, 1534–1542, doi:10.1175/1520-0426(2003)020.

Fujiwara, M., S.-P. Xie, M. Shiotani, H. Hashizume, F. Hasebe, H. Vömel, S. J. Oltmans, and T. Watanabe (2003b), Upper tropospheric inversion and easterly jet in the tropics, *J. Geophys. Res.*, *108*(D24, 4796), doi:10.1029/2003JD003,928.

Fujiwara, M., et al. (2010), Seasonal to decadal variations of water vapor in the tropical lower stratosphere observed with balloon-borne cryogenic frost point hygrometers, *J. Geophys. Res.*, *115* (D18304), doi: 10.1029/2010JD014179.

Hasebe, F., M. Fujiwara, N. Nishi, M. Shiotani, H. Vömel, S. Oltmans, H. Takashima, S. Saraspriya, N. Komala, and Y. Inai (2007), In situ observations of dehydrated air parcels advected horizontally in the tropical tropopause layer of the western Pacific, *Atmos. Chem. Phys.*, *7*, 803–813, doi:10.5194/acp-7-803-2007.

Hatsushika, H., and K. Yamazaki (2003), Stratospheric drain over Indonesia and dehydration within the tropical tropopause layer diagnosed by air parcel trajectories, *J. Geophys. Res.*, *180*D19, 4610, doi: 10.1029/2002JD002986.

Highwood, E. J., and B. J. Hoskins (1998), The tropical tropopause, *Q. J. R. Meteorol. Soc.*, *124*, 1579–1604.

Holton, J. R., P. H. Haynes, M. E. McIntyre, A. R. Douglass, R. B. Rood, and L. Pfister (1995), Stratosphere-troposphere exchange, *Rev. Geophys.*, *33*(4), 403–439.

Hoogen, R., V. V. Rozanov, and J. P. Burrows (1999), Ozone profiles from GOME satellite data: Algorithm description and first validation, *J. Geophys. Res.*, *104*(D7), 8263–8280, doi:10.1029/1998JD100093.

Jiang, Y. B., et al. (2007), Validation of Aura Microwave Limb Sounder ozone by ozonesonde and lidar measurements, *J. Geophys. Res.*, *112* (D24S34), doi:10.1029/2007JD008776.

Kanamitsu, M., W. Ebisuzaki, J. Woollen, S.-K. Yang, J. J. Hnilo, M. Fiorino, and G. L. Potter (2002), NCEP-DOE AMIP-II Reanalysis (R-2), *Bull. Am. Meteorol. Soc.*, *83*, 1631–1643, doi:10.1175/BAMS-83-11-1631.

Konopka, P., J.-U. Grooss, G. Gunther, F. Ploeger, R. Pommrich, R. Muller, and N. Livesey (2010), Annual cycle of ozone at and above the tropical tropopause: Observations versus simulations with the Chemical Lagrangian Model of the Stratosphere (CLaMS), *Atmos. Chem. Phys.*, *10*, 121–132, doi:10.5194/acp-10-121-2010.

Kroon, M., J. F. de Haan, J. P. Veefkind, L. Froidevaux, R. Wang, R. Kivi, and J. J. Hakkarainen (2011), Validation of operational ozone profiles from the Ozone Monitoring Instrument, *J. Geophys. Res.*, *116*(D18305), doi:10.1029/2010JD015100.

Liebmann, B., and C. A. Smith (1996), Description of a complete (interpolated) outgoing longwave radiation dataset, *Bull. Am. Meteorol. Soc.*, *77*(6), 1275–1277.

Livesey, N. J., W. V. Snyder, W. G. Read, and P. Wagner (2006), Retrieval algorithms for the EOS Microwave Limb Sounder (MLS) instrument, *IEEE Trans. Geosci. Remote Sens.*, *44* (5), 1144–1155, doi:10.1109/TGRS.2006.872327.

Livesey, N. J., et al. (2007), Earth Observing System (EOS) Aura Microwave Limb Sounder (MLS) Version 2.2 Level 2 data quality and description document, version 2.2x-1.0a.

Logan, J. A., et al. (2012), Changes in ozone over Europe: Analysis of ozone measurements from sondes, regular aircraft (MOZAIC) and alpine surface sites, *J. Geophys. Res.*, *117*(D09301), doi:10.1029/2011JD016952.

Mieruch, S., et al. (2012), Global and long-term comparison of SCIAMACHY limb ozone profiles with correlative satellite data (2002–2008), *Atmos. Meas. Tech.*, *5*(4), 771–788, doi:10.5194/amt-5-771-2012.

Nodzu, M. I., S.-Y. Ogino, Y. Tachibana, and M. D. Yamanaka (2006), Climatological description of seasonal variations in lower-tropospheric temperature inversion layers over the Indochina Peninsula, *J. Climate*, *19*, 3307–3319, doi:10.1175/JCLI3792.1.

Nodzu, M. I., S.-Y. Ogino, and M. D. Yamanaka (2011), Seasonal changes in a vertical thermal structure producing stable lower-troposphere layers over the inland region of the Indochina Peninsula, *J. Climate*, *24*, 3211–3223, doi:10.1175/2010JCLI3871.1.

Ogino, S.-Y., M. I. Nodzu, Y. Tachibana, J. Matsumoto, M. D. Yamanaka, and A. Watanabe (2010), Temperature inversions over the inland Indochina revealed by GAME-T enhanced rawinsonde observations, *SOLA*, *6*, 5–8, doi:10.2151/sola.2010-002.

Park, M., W. J. Randel, A. Gettelman, S. T. Massie, and J. H. Jiang (2007), Transport above the Asian summer monsoon anticyclone inferred from Aura Microwave Limb Sounder tracers, *J. Geophys. Res.*, *112*(D16309), doi:10.1029/2006JD008,294.

Pochanart, P., J. Kreasuwun, P. Sukasem, W. Geeratithadaniyom, M. S. Tabucanon, J. Hirokawa, Y. Kajii, and H. Akimoto (2001), Tropical tropospheric ozone observed in Thailand, *Atmos. Environ.*, *35*, 2657–2668.

Postel, G. A., and M. H. Hitchman (1999), A climatology of Rossby wave breaking along the subtropical tropopause, *J. Atmos. Sci.*, *56*, 359–373.

Randel, W. J., and M. Park (2006), Deep convective influence on the Asian summer monsoon anticyclone and associated tracer variability with AIRS, *J. Geophys. Res.*, *111*(D12314), doi:10.1029/2005JD006,490.

Seo, K.-H., and K. P. Bowman (2001), A climatology of isentropic cross-tropopause exchange, *J. Geophys. Res.*, *106*(D22), 28,159–28,172, doi: 10.1029/2000JD000295.

Shine, K. P., and P. M. de F. Forster (1999), The effect of human activity on radiative forcing of climate change: A review of recent developments, *Global Planet. Change*, *20*, 205–225

Shiotani, M., and F. Hasebe (1994), Stratospheric ozone variations in the equatorial region as seen in Stratospheric Aerosol and Gas Experiment data, *J. Geophys. Res.*, *99*, 14,575–14,584.

Smit, H. G. J., et al. (2007), Assessment of the performance of ECC-ozonesondes under quasi-flight conditions in the environmental simulation chamber: Insights from the Juelich Ozone Sonde Intercomparison Experiment (JOSIE), *J. Geophys. Res.*, *112*(D19306), doi: 10.1029/2006JD007308.

Solomon, S., D. Qin, M. Manning, Z. Chen, M. Marquis, K. B. Averyt, M. Tignor, and H. L. Miller (eds.) (2007), *IPCC, 2007: Climate Change 2007: The Physical Science Basis. Contribution of Working Group I to the Fourth Assessment Report of the Intergovernmental Panel on Climate Change*, 996 pp., Cambridge University Press, Cambridge.

Stohl, A., H. Wernli, P. James, M. Bourqui, C. Forster, M. A. Liniger, P. Seibert, and M. Sprenger (2003), A new perspective of stratosphere-troposphere exchange, *Bull. Am. Meteorol. Soc.*, *84*, 1565–1573, doi:10.5194/acp-6-4057-2006.

Stolarski, R. S., and S. M. Frith (2006), Search for evidence of trend slow-down in the long-term TOMS/SBUV total ozone data record:

The importance of instrument drift uncertainty, *Atmos. Chem. Phys.*, *6*, 4057–4065, doi:10.5194/acp-6-4057-2006.

Tanimoto, H., Y. Sawa, H. Matsueda, I. Uno, T. Ohara, K. Yamaji, J. Kurokawa, and S. Yonemura (2005), Significant latitudinal gradient in the surface ozone spring maximum over East Asia, *Geophys. Res. Lett.*, *32*(L21805), doi:10.1029/2005GL023514.

Tarasick, D. W., V. E. Fioletov, D. I. Wardle, J. B. Kerr, and J. Davies (2005), Changes in the vertical distribution of ozone over Canada from ozonesondes: 1980–2001, *J. Geophys. Res.*, *110* (D02304), doi: 10.1029/2004JD004643.

Thompson, A. M., et al. (2003a), Southern Hemisphere Additional Ozonesondes (SHADOZ) 1998–2000 tropical ozone climatology 1. Comparison with Total Ozone Mapping Spectrometer (TOMS) and ground-based measurements, *J. Geophys. Res.*, *108* (D2, 8238), doi: 10.1029/2001JD000967.

Thompson, A. M., et al. (2003b), Southern Hemisphere Additional Ozonesondes (SHADOZ) 1998–2000 tropical ozone climatology 2. Tropospheric variability and the zonal wave-one, *J. Geophys. Res.*, *108*(D2, 8241), doi:10.1029/2002JD002241.

Thompson, A. M., J. C. Witte, H. G. J. Smit, S. J. Oltmans, B. J. Johnson, V. W. J. H. Kirchhoff, and F. J. Schmidlin (2007), Southern Hemisphere Additional Ozonesondes (SHADOZ) 1998–2004 tropical ozoneclimatology: 3. Instrumentation, station-to-station variability, and evaluation with simulated flight profiles, *J. Geophys. Res.*, *112* (D03304), doi: 10.1029/2005JD007042.

Thompson, A. M., et al. (2012), SHADOZ (Southern Hemisphere Additional Ozonesondes) ozone climatology (2005-2009): Tropospheric and tropical tropopause layer (TTL) profiles with comparisons to OMI-based ozone products, *J. Geophys. Res.*, *117*(D23301), doi: 10.1029/2011JD016911.

Vömel, H., et al. (2007), Validation of Aura Microwave Limb Sounder water vapor by balloonborne cryogenic frost point hygrometer measurements, *J. Geophys. Res.*, *112* (D24S37), doi:10.1029/2007JD008, 698.

WMO (World, Meteorological Organization) (2011), *Scientific Assessment of Ozone Depletion: 2010, Global Ozone Research and Monitoring Project–Report No. 52*, 516 pp., World Meteorological Organization, Geneva, Switzerland

Worden, H. M., et al. (2007), Comparisons of Tropospheric Emission Spectrometer (TES) ozone profiles to ozonesondes: Methods and initial results, *J. Geophys. Res.*, *112*(D03309), doi:10.1029/2006JD007258.